International Journal of Nanomedicine

Dovepress
open access to scientific and medical research

Open Access Full Text Article

ORIGINAL RESEARCH

In vitro and in vivo protein release and anti-ischemia/reperfusion injury properties of bone morphogenetic protein-2-loaded glycyrrhetinic acid-poly(ethylene glycol)-b-poly(L-lysine) nanoparticles

This article was published in the following Dove Press journal:
International Journal of Nanomedicine
17 October 2017
Number of times this article has been viewed

Fang Shan[1]
YuJuan Liu[1]
Haiying Jiang[2]
Fei Tong[2]

[1]Department of Physiology, Hexi University Medical College, Zhangye, [2]Department of Pathology and Pathophysiology, Provincial Key Discipline of Pharmacology, Jiaxing University Medical College, Jiaxing, People's Republic of China

Abstract: Here, we describe a bone morphogenetic protein-2 (BMP-2) nanocarrier based on glycyrrhetinic acid (GA)-poly(ethylene glycol) (PEG)-b-poly(L-lysine) (PLL). A protein nanocarrier was synthesized, characterized and evaluated as a BMP-2 delivery system. The designed nanocarrier was synthesized based on the ring-opening polymerization of amino acid N-carboxyanhydride. The final product was measured with ^{1}H nuclear magnetic resonance. GA-PEG-b-PLL nanocarrier could combine with BMP-2 through electrostatic interaction to form polyion complex (PIC) micelles. BMP-2 could be rapidly and efficiently encapsulated through the GA-PEG-b-PLL nanocarrier under physiological conditions, exhibiting efficient encapsulation and sustained release. In addition, the GA-PEG-b-PLL-mediated BMP-2 delivery system could target the liver against hepatic diseases as it has GA-binding receptors. The anti-hepatic ischemia/reperfusion injury (anti-HI/RI) effect of BMP-2/GA-PEG-b-PLL PIC micelles was investigated in rats using free BMP-2 and BMP-2/PEG-b-PLL PIC micelles as controls, and the results showed that BMP-2/GA-PEG-b-PLL PIC micelles indicated significantly enhanced anti-HI/RI property compared to BMP-2 and BMP-2/PEG-b-PLL. All results suggested that GA-PEG-b-PLL could be used as a potential BMP-2 nanocarrier.

Key words: GA-PEG-b-PLL, PIC micelles, BMP-2, HI/RI

Introduction

Hepatic ischemia/reperfusion injury (HI/RI) is a pathophysiological phenomenon observed in various clinical settings, such as liver operations, liver transplantation, hemorrhagic shock and trauma.[1–5] The mechanisms involved in HI/RI range from oxidative stress, energy depletion and the activation of deleterious inflammatory mediators to cellular death.[6–9] Bone morphogenetic protein (BMP) 2 is a member of BMP family which belongs to transforming growth factor-β (TGF-β) involved in embryogenesis and morphogenesis of several tissues and organs.[10–14] Conventional BMP-2 therapy alleviates ischemia/reperfusion (I/R) injury (heart, kidney).[15,16] However, poor permeability, poor bioavailability and short half-life of BMP-2 restrict its use.[17] To overcome these defects, many delivery systems such as liposomes, hydrogels, polymeric nanoparticles and polyion complex (PIC) micelles have been formed.[18–34] These delivery systems can not only heighten the bioavailability of BMP-2 but also prolong its half-life and enhance its anti-IR injury properties.

Correspondence: Fei Tong
Department of Pathology and Pathophysiology, Provincial Key Discipline of Pharmacology, Jiaxing University Medical College, No 118 Jia Hang Road, Nanhu District, Jiaxing, Zhejiang 314001, People's Republic of China
Tel +86 137 3643 1280
Email tongxuchang@163.com

submit your manuscript | www.dovepress.com
Dovepress
http://dx.doi.org/10.2147/IJN.S146546

Among many protein delivery systems, PIC micelle has attained rapid development in the past decades. PIC micelle combines with oppositely charged protein by electrostatic interactions under mild conditions.[35–38] The loaded protein can avoid rapid degradation in vivo. Glycyrrhetinic acid (GA) has been affirmed to possess affluent receptors with high affinity on hepatocyte membrane.[39] Many studies have shown that the target site of GA is expressed highly in hepatoma carcinoma cells than the nontumor hepatocytes, and GA can be combined with functionalized hepatoma carcinoma cell-targeting drug carrier, including PIC micelle, to enhance the anti-hepatoma carcinoma cell properties as a ligand.[40,41]

In this paper, we report GA-poly(ethylene glycol) (PEG)-b-poly(L-lysine) (PLL) as a potential BMP-2 carrier. The designed GA-PEG-b-PLL was composed of GA-PEG and PLL (Scheme 1). Under physiological conditions (pH 7.4), GA-PEG-b-PLL was combined with BMP-2 (isoelectric point =4.8–5.1) to form PIC micelles via electrostatic interactions between positively charged PLL and negatively charged BMP-2. In this study, the encapsulation of BMP-2 in the PIC micelles, the release of BMP-2 from the PIC micelles, as well as the anti-hepatic ischemia/reperfusion injury (anti-HI/RI; Scheme 2) effect of the PIC micelles were measured using PEG-b-PLL as control polymers.

Materials and methods

Materials

GA was bought from Jinzhu Pharmaceutical Co., Ltd. (Nanjing, People's Republic of China). H_2N-PEG-NH_2 (molecular weight =5,000 Da) was purchased from Aladdin (Shanghai, People's Republic of China). BMP-2 was bought from Beijing Baiying Biological Science and Technology Co Ltd. L-02 cells were purchased from Shanghai Yansheng Industrial Co. Ltd. Other reagents were purchased from Sigma.

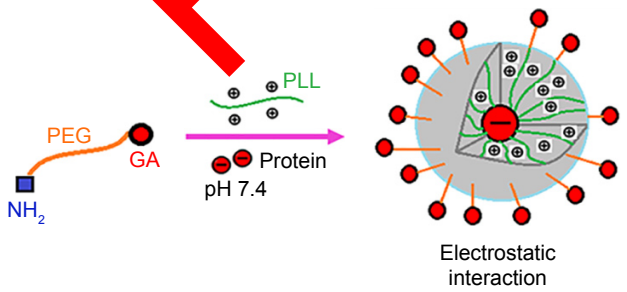

Scheme 1 The structure of BMP-2/GA-PEG-b-PLL.
Abbreviations: BMP-2, bone morphogenetic protein-2; GA, glycyrrhetinic acid; PEG, poly(ethylene glycol); PLL, poly(L-lysine).

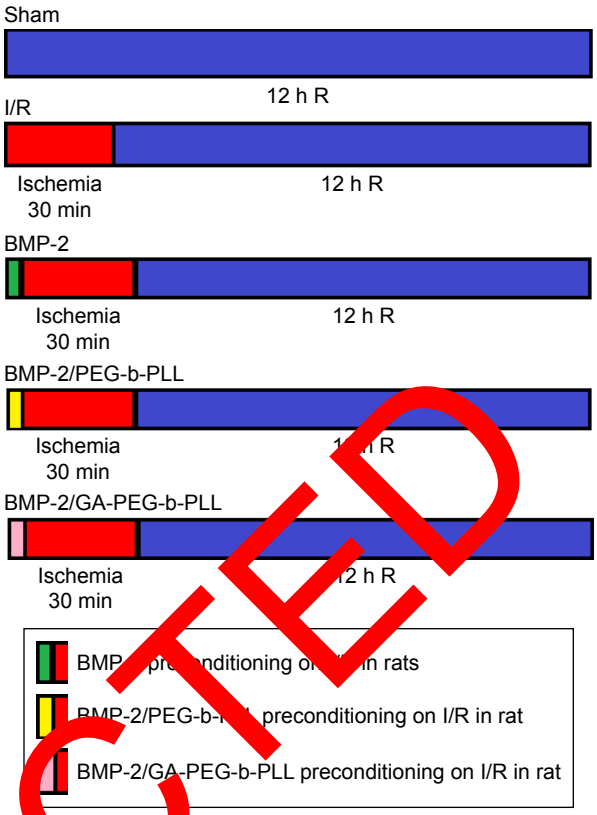

Scheme 2 The effect of BMP-2/GA-PEG-b-PLL on HI/RI.
Abbreviations: BMP-2, bone morphogenetic protein-2; GA, glycyrrhetinic acid; PEG, poly(ethylene glycol); PLL, poly(L-lysine); HI/RI, hepatic ischemia/reperfusion injury; I/R, ischemia/reperfusion.

Methods

Synthesis of GA-PEG-NH_2

GA-PEG-NH_2 was synthesized by following previous literature.[39] The detailed method is shown in the Supplementary material.

Synthesis of PEG-b-PLL

PEG-b-PLL was synthesized by ring-opening polymerization of ε-benzyloxycarbonyl-L-lysine N-carboxyanhydride (ZLL-NCA) with PEG-NH_2 as macroinitiator. A suitable quantity of PEG-NH_2 in N,N-dimethylformamide (DMF) was mixed with ZLL-NCA/DMF fluid by vacuumization and N_2 protection. The mixture was stirred at 30°C for 72 h and dialyzed for 72 h. The PEG-b-PLL polymeric compound was obtained via freeze drying. The degree of polymerization of PLL was 50, and the final product was characterized through ^{1}H nuclear magnetic resonance (NMR).

Synthesis of GA-PEG-b-PLL

GA-PEG-b-PLL was synthesized by ring-opening polymerization of ZLL-NCA with GA-PEG-NH_2 as macroinitiator.

A suitable quantity of GA-PEG-NH_2 in DMF was mixed with ZLL-NCA/DMF fluid by vacuumization and N_2 protection. The mixture was stirred at 30°C for 72 h and dialyzed for 72 h. The GA-PEG-b-PLL polymeric compound was obtained via freeze drying. The degree of polymerization of PLL was 50.

Cytotoxicity assessment of PEG-b-PLL and GA-PEG-b-PLL

A detailed depiction of the assessment of cytotoxicity (L-02 cells were selected) of PEG-b-PLL and GA-PEG-b-PLL is provided in our previous work.[42]

Encapsulation of BMP-2 into PEG-b-PLL and GA-PEG-b-PLL

To evaluate the BMP-2-loading efficiency of PEG-b-PLL, 5 mg/mL BMP-2 in phosphate-buffered solution (PBS; pH 7.2, 0.01 mmol/L) was mixed with PEG-b-PLL in PBS, and then the resulting solution was placed into a dialysis bag (MWCO =7,000 Da) and dialyzed. The PEG-b-PLL-loaded BMP-2 was evaluated using ELISA kit and transmission electron microscopy (TEM). Encapsulation of BMP-2 into GA-PEG-b-PLL was performed using the loading method described above.

BMP-2 release in vitro

Release of BMP-2 from PEG-b-PLL and GA-PEG-b-PLL was verified by dialysis method (MWCO =10,000 Da) at 37°C, with 5 mL of BMP-2-loaded PEG-b-PLL and GA-PEG-b-PLL against PBS. The BMP-2/PEG-b-PLL and BMP-2/GA-PEG-b-PLL complexes were prepared via encapsulation of BMP-2 with PEG-b-PLL and GA-PEG-b-PLL, respectively. After a specific time interval, a given volume of the release media was extracted and supplemented with an equal volume of fresh release media. The amount of BMP-2 released was measured by ELISA method.

In vitro transfection

L-02 cells with DMEM containing 10% fetal bovine serum were cultured. Twenty-four hours before transfection, cells were inoculated in a 24-well culture plate (1×10^5 per hole). When transfected cells reached 70% fusion, these were rinsed two times with PBS, and PEG-b-PLL/pEGFP and GA-PEG-b-PLL/pEGFP culture medium was added to each hole without serum. After culturing for 4 h in 5% CO_2 under 37°C, the medium was removed, and cells were rinsed two times with PBS. Then, 1 mL of culture medium containing 10% fetal bovine serum was added, and the cells were cultured for 24 h. After 24 h, pEGFP expression was observed using an inverted fluorescence microscope.

Assessment of blood BMP-2 concentration

Male SD rats (20–25 g) were administrated 4 μg/kg BMP-2 or BMP-2/PEG-b-PLL via abdominal subcutaneous injection. About 0.2 mL blood was extracted at a specified time interval and separated immediately via centrifugation (12,000× *g* for 15 min at 4°C). The concentration of BMP-2 and BMP-2/PEG-b-PLL in rat blood was evaluated using ELISA kit.

Animal and surgical process of HI/RI

Male SD rats (20–25 g) were provided by Jiangxing University Medical College. All animal procedures were approved by the institutional ethics committee of Jiaxing University Medical College. The investigation conformed to the Guide for Care and Use of Laboratory Animals published by the US National Institutes of Health (updated in 2011). In this study, 50 male SD rats were assigned to five groups (each group had 10 rats): 1) Sham group; 2) I/R group (rats were anesthetized with 1% pentobarbital sodium [50 mg/kg] via intraperitoneal injection; the abdomina were opened, and the left and median liver lobes were exposed and clamped for 30 min in order to cause 70% hepatic ischemia, followed by 12 h of reperfusion); 3) BMP-2 group (rats were administrated BMP-2 once a day [4 μg/kg] via abdominal subcutaneous injection for 3 days prior to I/R procedures); 4) BMP-2/PEG-b-PLL group (rats were administrated BMP-2/PEG-b-PLL only once [4 μg/kg] via abdominal subcutaneous injection for 3 days prior to I/R procedures); and 5) BMP-2/GA-PEG-b-PLL group (rats were administrated BMP-2/GA-PEG-b-PLL only once [4 μg/kg] via abdominal subcutaneous injection for 3 days prior to I/R procedures).

Blood was collected from the abdominal aorta and centrifuged at 3,600× *g* for 15 min to gain the sera. Livers of male SD rats were collected and stored at −80°C until further analysis.

Histopathological assessment

Four-micrometer-thick sections of livers were cut and stained with hematoxylin and eosin. Each sample was blindly analyzed to measure the extent of liver damage based on the technique outlined by Yu et al.[43] Briefly, 24 regions of the liver were graded for the degree of injury based on each of the following parameters: cytoplasmic discoloration, vacuolation formation, nuclear pyknosis, nuclear fragmentation, nuclear discoloration and red cell stasis. Specifically, one whole deep coronal section was

evaluated under a microscope, and the extent of injury was graded based on the percentage of involvement of the liver. Higher scores represented more severe injury, with the maximum score being 4 (0, histopathological changes <10%; 1, 10%–25%; 2, 25%–50%; 3, 50%–75%; and 4, 75%–100%). The mean score for each parameter was verified and subjected to statistical analysis.

Liver function assessment

Aspartate aminotransferase (AST) and alanine aminotransferase (ALT) were assessed using the previously described methods.[43] Blood was collected after reperfusion for 12 h and centrifuged at 3,600× *g* for 15 min to get the sera, following which AST and ALT activities were measured by a standard automatic biochemistry analyzer.

Superoxide dismutase (SOD) activity and malonyldialdehyde (MDA) level assessment

Blood was collected after reperfusion for 12 h and centrifuged at 3,600× *g* for 15 min to gain the sera. SOD activity and MDA levels were measured using xanthine oxidase and thiobarbituric acid methods.[44] The absorbances were measured at 550 and 532 nm, respectively. Lipid peroxide levels were expressed as "U" of SOD/mL and "nmol" of MDA/mL.

Assessment of interleukin-6 (IL-6), tumor necrosis factor-α (TNF-α) and macrophage inflammatory protein-2 (MIP-2) levels

IL-6, TNF-α and MIP-2 levels were estimated using the previously reported methods.[45,46] Blood was collected after reperfusion for 12 h and centrifuged at 3,600× *g* for 15 min to gain the sera. IL-6, TNF-α and MIP-2 levels were measured using commercially available kits.

Assessment of proliferating cell nuclear antigen (Ki-67) expression

Five-micrometer thick sections of liver were acquired and mounted on PLL-coated slides.[47] The sections were immersed in 0.3% H_2O_2 for 20 min and washed with PBS. These were then incubated in rabbit anti-Ki-67 polyclonal antiserum for 1 h. After primary incubation and three rinses in PBS, sections were incubated in biotinylated goat anti-rabbit IgG for 10 min. Following the incubation in substrate chromagen solution for 10 min, all sections were washed in PBS and distilled water, mounted in glycerol and evaluated under a microscope. Liver sections that stained positively for Ki-67 were evaluated and compared among groups.

Western blot analysis

The methodology used had been described previously.[48–50] Briefly, liver tissues were homogenized in protein lysate buffer. The homogenate was resolved on polyacrylamide SDS gels and electrophoretically transferred to polyvinylidene difluoride membranes. The membranes were blocked with 3% BSA, incubated with primary antibodies against active Indian hedgehog (Ihh), sonic hedgehog (Shh), glioma-associated oncogene-1 (Gli-1) and subsequently with alkaline phosphatase-conjugated secondary antibodies. These were finally developed by adding 5-bromo-4-chloro-3-indolyl phosphate/nitroblue tetrazolium. Blots were stained with anti-β-actin antibody, and the levels of proteins were normalized with respect to β-actin and density.

Statistical analyses

All experiments were performed in triplicate unless otherwise noted. All data are expressed as mean ± standard deviation. Statistical analyses were carried out using ANOVA with post hoc testing, and data were analyzed using SPSS. A *p* value <0.01 denoted statistical significance.

Results

Synthesis of GA-PEG-NH_2

Synthesis of GA-PEG-NH_2 is depicted in the Supplementary material.

Synthesis and characterization of PEG-b-PLL

PEG-b-PLL consisted of PEG and PLL (Figure 1). In the current study, the molecular weight of PEG was 5,000 Da, and the degree of polymerization of PLL was 50. The procedure of its synthesis is depicted in Figure 1. The ^{1}H NMR spectrum of PEG-b-PLL is presented in Figure 2, and number-average molecular weight values are given in Table 1. The characteristic proton peak of both PEG and PLL was observed, corroborating that the synthesis proceeded in a controlled manner and was successful.

Synthesis and characterization of GA-PEG-b-PLL

GA-PEG-b-PLL consisted of GA-PEG and PLL (Figure 3). In the current study, the molecular weight of PEG was 5,000 Da, and the degree of polymerization of PLL was 50. The procedure of its synthesis is depicted in Figure 3.

Cellular viability assessment

Cellular toxicity due to PEG-b-PLL and GA-PEG-b-PLL in L-02 cells was assessed after 24-h culturing, and the result is described in Figure 4B. PEG-b-PLL and GA-PEG-b-PLL

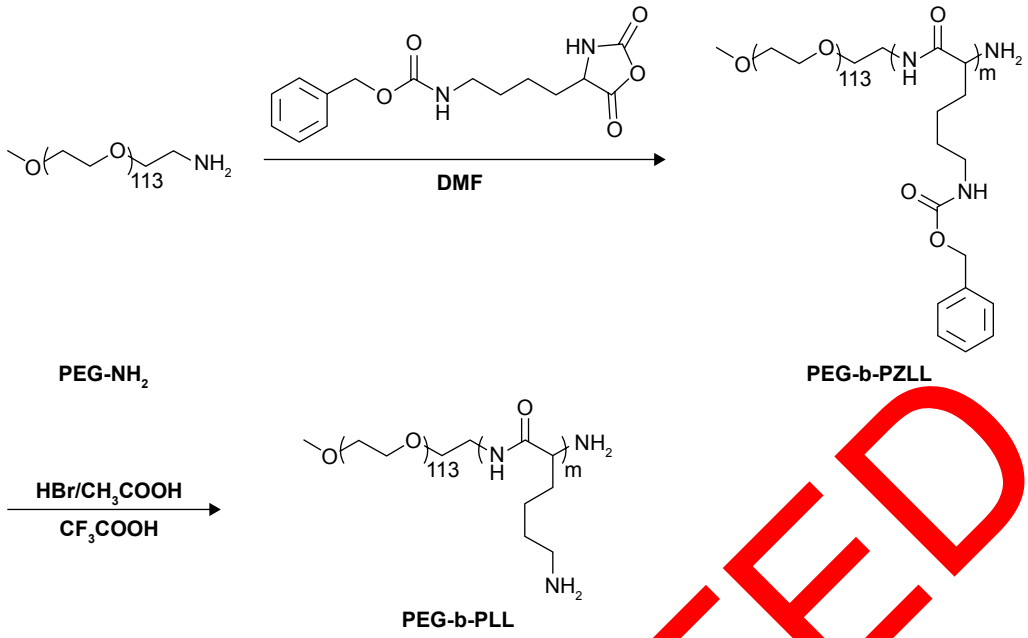

Figure 1 Synthesis of PEG-b-PLL.
Abbreviations: PEG, poly(ethylene glycol); PLL, poly(L-lysine); DMF, N,N-dimethylformamide; PZLL, poly(ε-benzyloxycarbonyl-L-lysine).

exerted low cellular toxicity even at a concentration as high as 300 μg/mL.

Encapsulating capacity of BMP-2 in PEG-b-PLL and GA-PEG-b-PLL

BMP-2 was found to be efficiently encapsulated in PEG-b-PLL at pH 7.4 due to electrostatic interaction. BMP-2 was added to PEG-b-PLL (mass ratio 1:5) and dialyzed (MWCO =7,000 Da) against PBS. The dialysis of free BMP-2 as a control was also conducted at pH 7.4 in PBS. To evaluate the encapsulation efficiency of BMP-2 in PEG-b-PLL, the quantity of BMP-2 in the dialysate was measured using ELISA kit and deducted from the total quantity of added BMP-2. The encapsulation efficiency of BMP-2 was found to be 5.78%, expressed as the mass ratio of encapsulated BMP-2 to the polymeric compound (Table 1). Loading capacity process of BMP-2 in GA-PEG-b-PLL was consistent with the loading capacity as above.

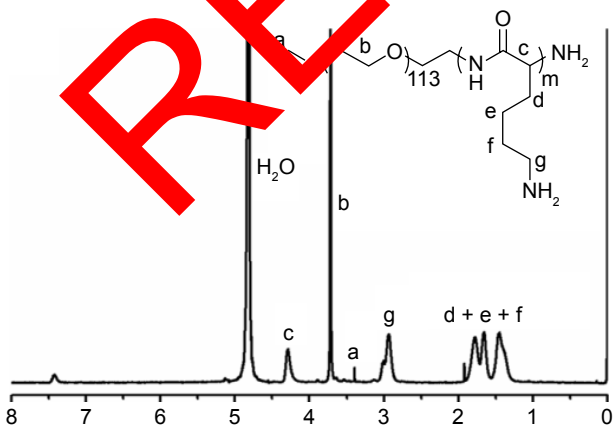

Figure 2 ^{1}H NMR spectra of PEG-b-PLL.
Abbreviations: ^{1}H NMR, ^{1}H nuclear magnetic resonance; PEG, poly(ethylene glycol); PLL, poly(L-lysine).

Characterization of BMP-2/PEG-b-PLL

BMP-2/PEG-b-PLL was assessed via TEM, and the image is shown in Figure 4A. BMP-2/PEG-b-PLL showed an orbicular structure, and the diameter was approximately 62 nm (Table 1).

In vitro release of BMP-2 from PEG-b-PLL and GA-PEG-b-PLL

The release of BMP-2 from PEG-b-PLL and GA-PEG-b-PLL was assessed using a dialysis method (MWCO =100,000 Da) at 37°C, with 5 mL of BMP-2-loaded PEG-b-PLL and GA-PEG-b-PLL. The cumulative release ratios of BMP-2

Table 1 Molecular weights, TEM and BMP-2-loading capacity of PEG-b-PLL

Sample	M_n (kDa)/ ^{1}H NMR	TEM (nm)	Loading capacity (%)
PEG-b-PLL	17.3	NA	NA
BMP-2/PEG-b-PLL	NA	62	5.78

Abbreviations: BMP-2, bone morphogenetic protein-2; ^{1}H NMR, ^{1}H nuclear magnetic resonance; M_n, number-average molecular weight; NA, not applicable; PEG, polyethylene glycol; PLL, poly(L-lysine); TEM, transmission electron microscopy.

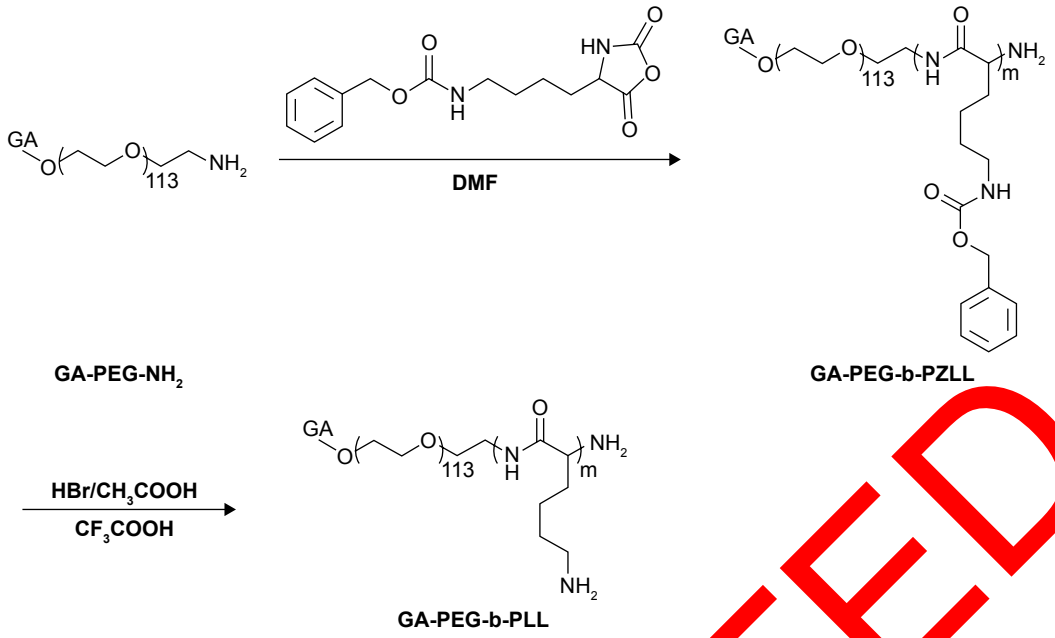

Figure 3 Synthesis of GA-PEG-b-PLL.
Abbreviations: DMF, N,N-dimethylformamide; GA, glycyrrhetinic acid; PEG, poly(ethylene glycol); PLL, poly(L-lysine); PZLL, poly(ε-benzyoxycarbonyl-L-lysine).

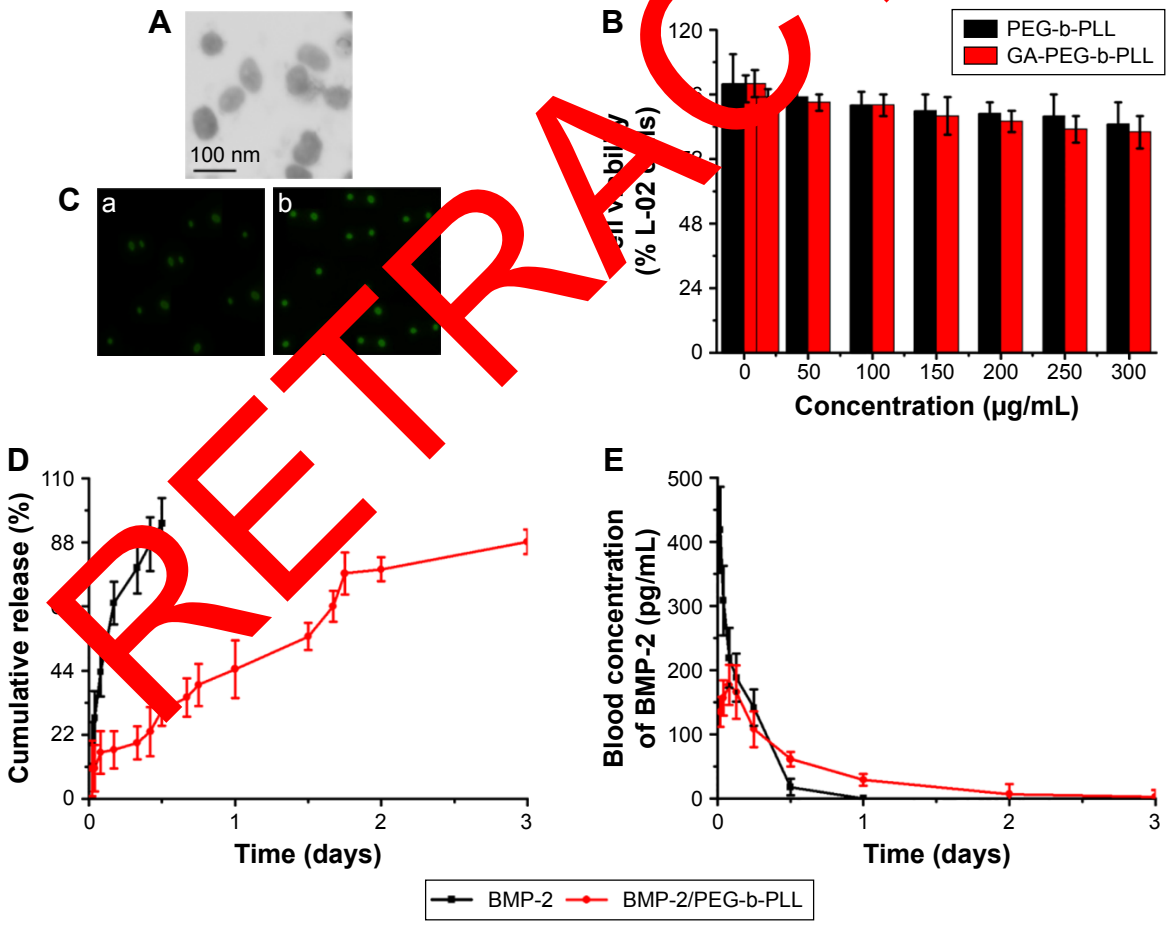

Figure 4 Characterization of PEG-b-PLL, GA-PEG-b-PLL and BMP-2/PEG-b-PLL.
Notes: (**A**) TEM image of BMP-2/PEG-b-PLL. (**B**) Cellular viability of L-02 cells cultured with different concentrations of PEG-b-PLL and GA-PEG-b-PLL. (**C**) In vitro transfection of PEG-b-PLL (a) and GA-PEG-b-PLL (b). (**D**) Cumulative release profile of free BMP-2 and BMP-2 from BMP-2/PEG-b-PLL. (**E**) Blood concentration of free BMP-2 and BMP-2 from BMP-2/PEG-b-PLL.
Abbreviations: BMP-2, bone morphogenetic protein-2; GA, glycyrrhetinic acid; PEG, polyethylene glycol; PLL, poly(L-lysine); TEM, transmission electron microscopy.

from BMP-2/PEG-b-PLL and BMP-2/GA-PEG-b-PLL are shown in Figure 4D. After 1 h, approximately 10.56% of the BMP-2 was released from BMP-2/PEG-b-PLL and BMP-2/GA-PEG-b-PLL, indicative of an initial burst release of BMP-2. Approximately 88.24% of the BMP-2 was released after 3 days.

In vitro transfection

Using pEGFP as reporter gene, the transfection efficiency of PEG-b-PLL and GA-PEG-b-PLL in L-02 cells was assessed (Figure 4C). Under serum-free conditions, the transfection efficiency of PEG-b-PLL was the lowest, and the transfection efficiency of GA-PEG-b-PLL was the highest.

Plasma BMP-2 concentration

Pharmacodynamic research showed that, in rats treated with BMP-2 solution, plasma BMP-2 concentrations augmented fast, reaching the peak within 0.5 h (418.7 pg/mL), followed by a remarkable decline after 24 h (0 pg/mL; Figure 4E). In contrast, the concentration of the BMP-2/PEG-b-PLL complex gradually peaked within 2 h (176.5 pg/mL) and remained at a comparatively low level by 3 days (1.9 pg/mL on day 3; Figure 4E).

Histopathological assessment

Light microscopy image of liver section is shown in Figure 5. The hepatic lobule structure disorder, hepatic sinusoids and central vein had different degrees of blood stasis and liver blood sinus narrowed or disappeared. Endothelial cells and hepatocytes generally showed edema and degeneration, neutrophil attachment and focal necrosis. Cytoplasmic discoloration, vacuole formation, nuclear pyknosis, nuclear fragmentation, nuclear discoloration and red cell stasis were observed in histological specimens from the I/R group (Figure 5Ab) but were absent in the Sham group (Figure 5Aa). Histological alteration was alleviated in specimens from the BMP-2- and BMP-2/PEG-b-PLL-treated groups (Figure 5Ac and d) compared to the I/R group. Histological alteration was significantly alleviated in specimens from the BMP-2/GA-PEG-b-PLL-treated groups (Figure 5Ae) compared to the I/R group. The corresponding quantitative analysis is shown in Figure 5B.

Estimation of ALT and AST levels

Contents of ALT and AST were measured after reperfusion for 12 h (Figure 6A), and were higher in the I/R group than in the Sham group ($p<0.01$; ALT: Sham group 342.51±68.91 U/L, I/R group 6,782.34±71.26 U/L; AST: Sham group 278.92±70.23 U/L, I/R group 9,125.61±89.88 U/L). Administration of BMP-2 decreased ALT (5,023.26±76.76 U/L) and AST (8,134.54±62.34 U/L) compared with ALT and AST in the I/R group ($p<0.01$). Administration of BMP-2/PEG-b-PLL decreased ALT (4,321.57±69.87 U/L) and AST (6,753.29±91.32 U/L) compared with ALT and AST in the I/R group ($p<0.01$). Administration of BMP-2/GA-PEG-b-PLL significantly decreased ALT (3,892.59±83.45 U/L) and AST (5,321.53±58.85 U/L) compared with ALT and AST in the I/R group ($p<0.01$).

Estimation of SOD activity and MDA level

Activity of SOD was measured after reperfusion for 12 h (Figure 6B), and was lower in the I/R group than in the Sham group ($p<0.01$; Sham group 115.67±6.64 U/mL, I/R group 43.69±5.49 U/mL). Administration of BMP-2 increased SOD

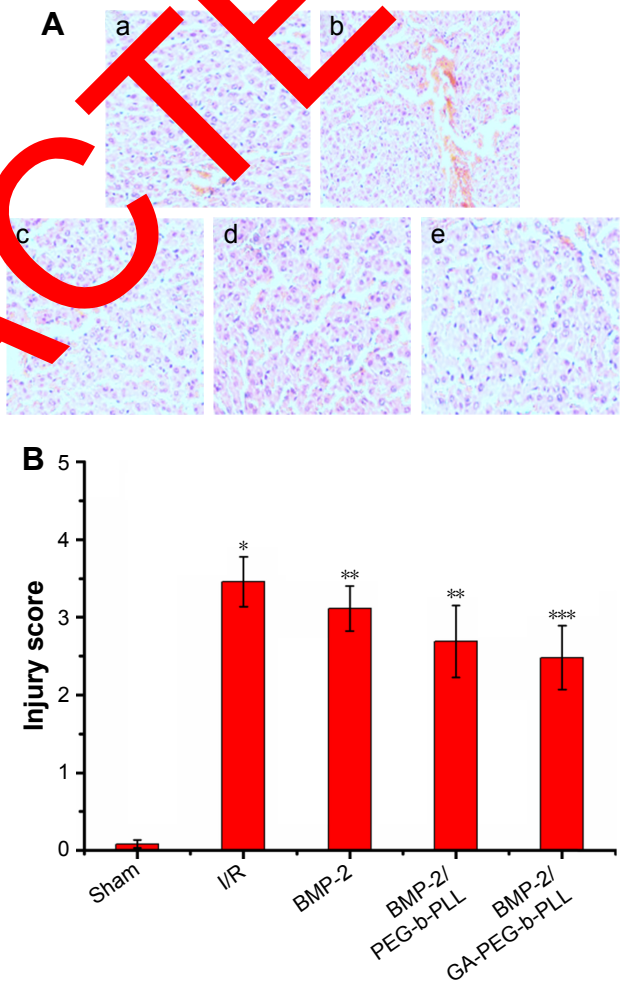

Figure 5 Histopathological assessment of liver damage.
Notes: (**A**) Light microscope images (×100) obtained from (a) Sham group, (b) I/R group, (c) BMP-2 group, (d) BMP-2/PEG-b-PLL group and (e) BMP-2/GA-PEG-b-PLL group. (**B**) Quantitative injury scores, expressed as the mean ± SD. A significant increase relative to the Sham group is denoted by * ($p<0.01$), a significant decrease relative to the I/R group is denoted by ** ($p<0.01$) and a significant decrease relative to the I/R group is denoted by *** ($p<0.01$).
Abbreviations: BMP-2, bone morphogenetic protein-2; GA, glycyrrhetinic acid; I/R, ischemia/reperfusion; PEG, poly(ethylene glycol); PLL, poly(L-lysine); SD, standard deviation.

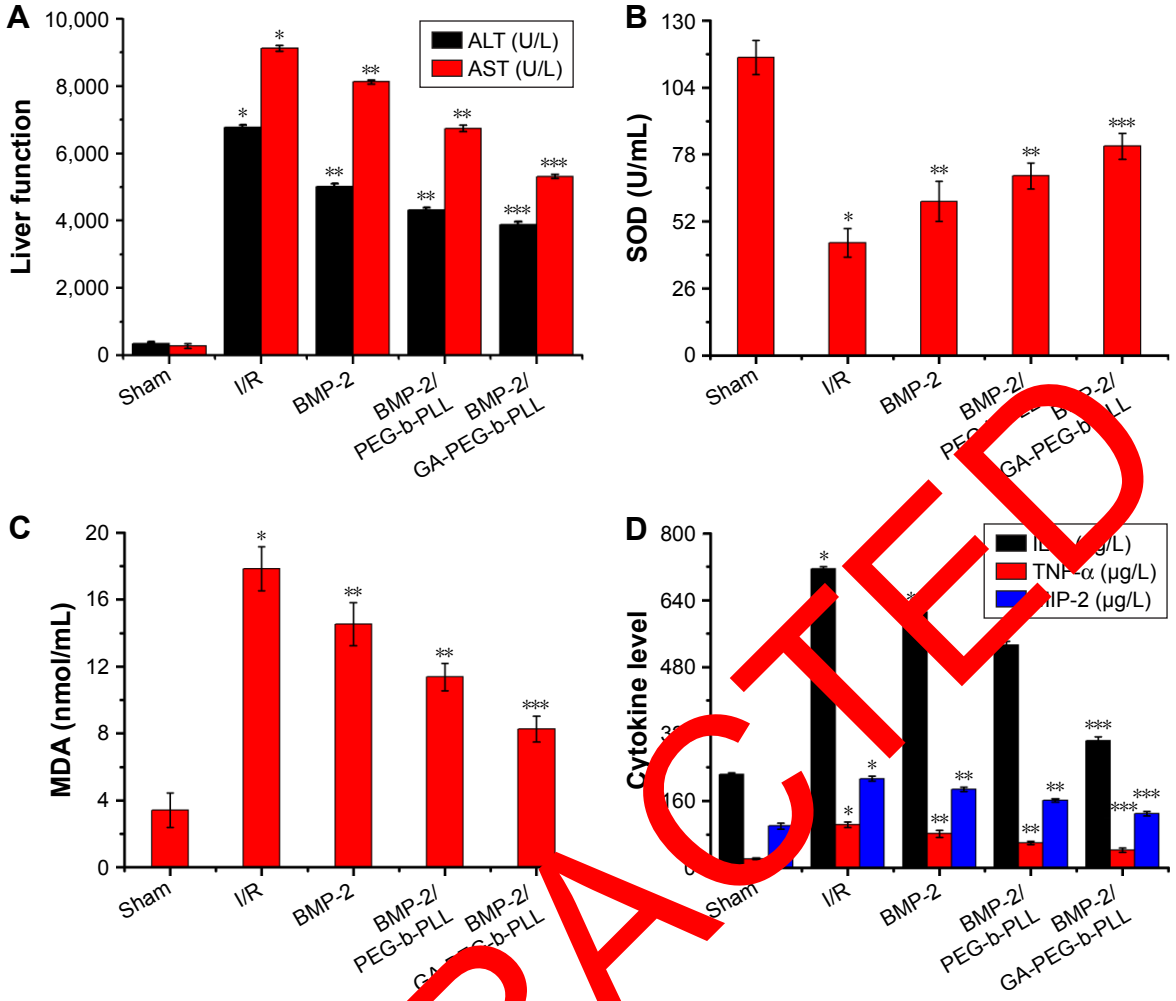

Figure 6 The activities of ALT, AST and SOD and the levels of MDA, IL-6, TNF-α and MIP-2 in HI/RI in different groups of rats.

Notes: The blood of rats in Sham, I/R, BMP-2, BMP-2/PEG-b-PLL and BMP-2/GA-PEG-b-PLL groups was collected 12 h after reperfusion, and the activities of ALT, AST and SOD and the levels of MDA, IL-6, TNF-α and MIP-2 were measured. Results are expressed as mean ± SD. (**A**) A significant increase from Sham group is denoted by * ($p<0.01$), a significant decrease from I/R group is denoted by ** ($p<0.01$) and a significant decrease from I/R group is denoted by *** ($p<0.01$). (**B**) A significant decrease from Sham group is denoted by * ($p<0.01$), a significant increase from I/R group is denoted by ** ($p<0.01$) and a significant increase from I/R group is denoted by *** ($p<0.01$). (**C**) A significant increase from Sham group is denoted by * ($p<0.01$), a significant decrease from I/R group is denoted by ** ($p<0.01$) and a significant decrease from I/R group is denoted by *** ($p<0.01$). (**D**) A significant increase from Sham group is denoted by * ($p<0.01$), a significant decrease from I/R group is denoted by ** ($p<0.01$) and a significant decrease from I/R group is denoted by *** ($p<0.01$).

Abbreviations: ALT, alanine aminotransferase; AST, aspartate aminotransferase; BMP-2, bone morphogenetic protein-2; GA, glycyrrhetinic acid; HI/RI, hepatic ischemia/reperfusion injury; IL-6, interleukin-6; I/R, ischemia/reperfusion; MDA, malonyldialdehyde; MIP-2, macrophage inflammatory protein-2; PEG, poly(ethylene glycol); PLL, poly(L-lysine); SD, standard deviation; SOD, superoxide dismutase; TNF-α, tumor necrosis factor-α.

(59.81±7.8[illegible] U/mL) compared with SOD in the I/R group ($p<0.01$). Administration of BMP-2/PEG-b-PLL increased SOD (69.74±4.99 U/mL) compared with SOD in the I/R group ($p<0.01$). Administration of BMP-2/GA-PEG-b-PLL significantly increased SOD (81.26±5.07 U/mL) compared with SOD in the I/R group ($p<0.01$).

Content of MDA was measured after reperfusion for 12 h (Figure 6C), and was higher in the I/R group than in the Sham group ($p<0.01$; Sham group 3.42±1.02 nmol/mL, I/R group 17.84±1.31 nmol/mL). Administration of BMP-2 decreased MDA (14.58±1.29 nmol/mL) compared with MDA in the I/R group ($p<0.01$). Administration of BMP-2/PEG-b-PLL decreased MDA (11.38±0.82 nmol/mL) compared with MDA in the I/R group ($p<0.01$). Administration of BMP-2/GA-PEG-b-PLL significantly decreased MDA (8.27±0.76 nmol/mL) compared with MDA in the I/R group ($p<0.01$).

Estimation of IL-6, TNF-α and MIP-2 levels

Level of IL-6 was measured after reperfusion for 12 h (Figure 6D), and was higher in the I/R group than in the Sham group ($p<0.01$; Sham group 223.29±4.53 μg/L, I/R group 715.24±5.03 μg/L). Administration of BMP-2 decreased IL-6 (612.45±8.92 μg/L) compared with IL-6 in the I/R group

($p<0.01$). Administration of BMP-2/PEG-b-PLL decreased IL-6 (532.19±10.21 μg/L) compared with IL-6 in the I/R group ($p<0.01$). Administration of BMP-2/GA-PEG-b-PLL significantly decreased IL-6 (303.76±8.93 μg/L) compared with IL-6 in the I/R group ($p<0.01$).

Level of TNF-α was measured after reperfusion for 12 h (Figure 6D), and was higher in the I/R group than in the Sham group ($p<0.01$; Sham group 21.69±2.41 μg/L, I/R group 103.46±6.73 μg/L). Administration of BMP-2 decreased TNF-α (81.28±8.25 μg/L) compared with TNF-α in the I/R group ($p<0.01$). Administration of BMP-2/PEG-b-PLL decreased TNF-α (59.33±4.09 μg/L) compared with TNF-α in the I/R group ($p<0.01$). Administration of BMP-2/GA-PEG-b-PLL significantly decreased TNF-α (42.11±5.11 μg/L) compared with TNF-α in the I/R group ($p<0.01$).

Level of MIP-2 was measured after reperfusion for 12 h (Figure 6D), and was higher in the I/R group than in the Sham group ($p<0.01$; Sham group 99.83±7.13 μg/L, I/R group 213.39±6.29 μg/L). Administration of BMP-2 decreased MIP-2 (187.24±5.17 μg/L) compared with MIP-2 in the I/R group ($p<0.01$). Administration of BMP-2/PEG-b-PLL decreased MIP-2 (161.32±4.39 μg/L) compared with MIP-2 in the I/R group ($p<0.01$). Administration of BMP-2/GA-PEG-b-PLL significantly decreased MIP-2 (129.82±5.52 μg/L) compared with MIP-2 in the I/R group ($p<0.01$).

Estimation of Ki-67 expression

Expression of Ki-67 was measured after reperfusion for 12 h (Figure 7), and was higher in the I/R group than in the Sham group ($p<0.01$). Administration of BMP-2 increased Ki-67 expression compared with Ki-67 expression in the I/R group ($p<0.01$). Administration of BMP-2/PEG-b-PLL increased Ki-67 expression compared with Ki-67 expression in the I/R group ($p<0.01$). Administration of BMP-2/GA-PEG-b-PLL significantly increased Ki-67 expression compared with Ki-67 expression in the I/R group ($p<0.01$).

Estimation of Ihh, Shh and Gli-1 expressions

Expression of Ihh, Shh and Gli-1 expressions was measured after reperfusion for 12 h (Figure 8), and was higher in the I/R group than in the Sham group ($p<0.01$). Administration of BMP-2 increased Ihh, Shh and Gli-1 expressions compared with Ihh, Shh and Gli-1 expressions in the I/R group ($p<0.01$). Administration of BMP-2/PEG-b-PLL increased Ihh, Shh and Gli-1 expressions compared with Ihh, Shh and Gli-1 expressions in the I/R group ($p<0.01$). Administration of BMP-2/GA-PEG-b-PLL significantly increased Ihh, Shh and Gli-1 expressions compared with Ihh, Shh and Gli-1 expressions in the I/R group ($p<0.01$).

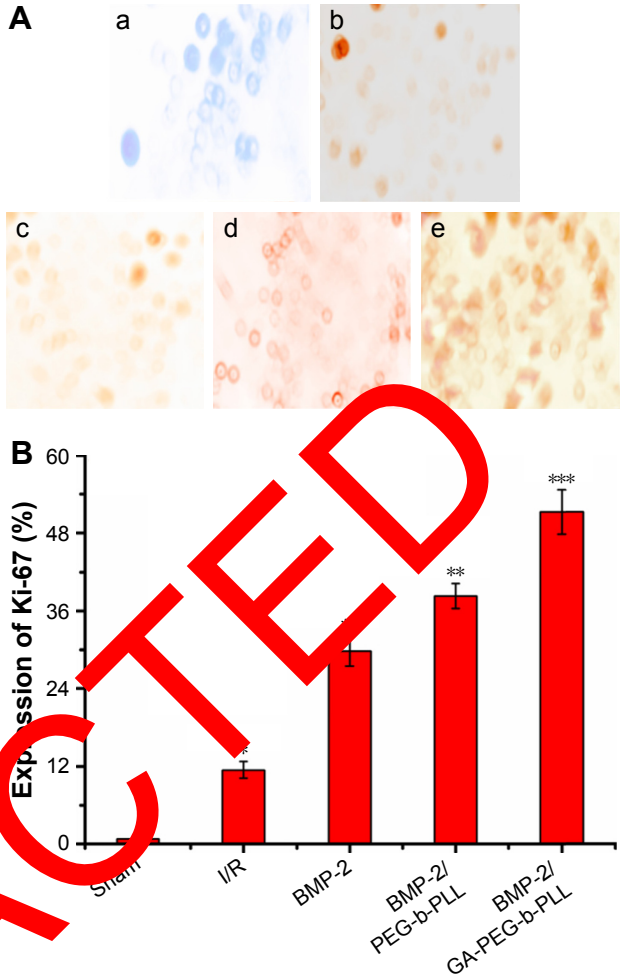

Figure 7 Expression of Ki-67 in HI/RI in different groups of rats.
Notes: (**A**) Ki-67 expression in (a) Sham group, (b) I/R group, (c) BMP-2 group, (d) BMP-2/PEG-b-PLL group and (e) BMP-2/GA-PEG-b-PLL group. (**B**) Quantitative Ki-67 expression, expressed as the mean ± SD. A significant increase relative to the Sham group is denoted by * ($p<0.01$), a significant increase relative to the I/R group is denoted by ** ($p<0.01$) and a significant increase relative to the I/R group is denoted by *** ($p<0.01$).
Abbreviations: BMP-2, bone morphogenetic protein-2; GA, glycyrrhetinic acid; HI/RI, hepatic ischemia/reperfusion injury; I/R, ischemia/reperfusion; Ki-67, proliferation cell nuclear antigen; PEG, poly(ethylene glycol); PLL, poly(L-lysine); SD, standard deviation.

Discussion

Higher liver cell uptake, specific liver accumulation in vivo and speedy hepatocyte protein drug release had been difficult to achieve while using PIC micelle as anti-HI/RI protein drug carrier in rats. To design a delivery system with active targeting and efficient stimuli-responsiveness has been promising.[40] BMP-2 is a member of the TGF-β superfamily of proteins and involved in abundant biological actions.[15] However, its poor bioavailability by fast clearance, poor permeability and

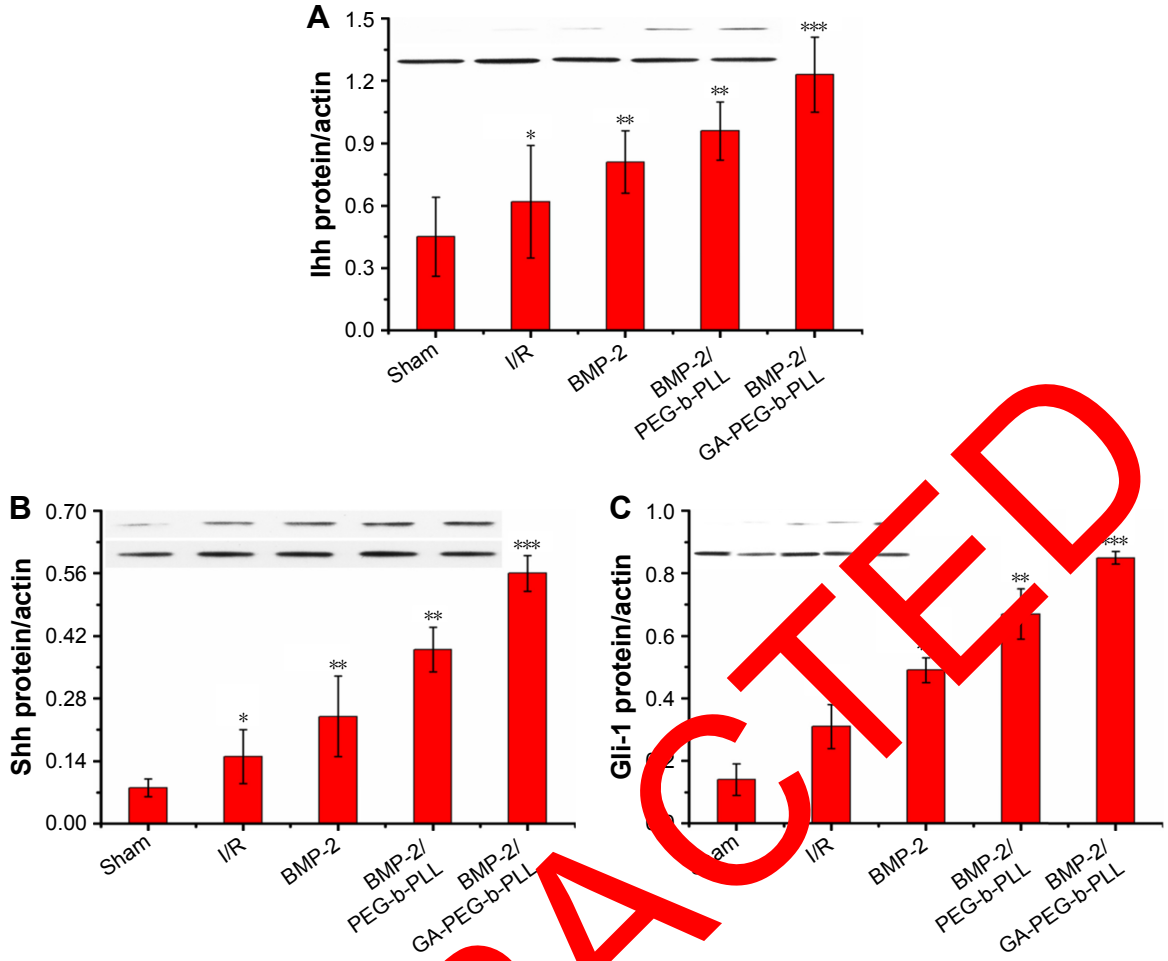

Figure 8 The qualitative expression and quantitative analyses of (**A**) Ihh, (**B**) Shh and (**C**) Gli-1 in HI/RI in different groups of rats.
Notes: The liver tissues of rats in Sham, I/R, BMP-2, BMP-2/PEG-b-PLL and BMP-2/GA-PEG-b-PLL groups were collected 12 h after reperfusion, and the expressions of Ihh, Shh and Gli-1 were measured. Results are expressed as mean ± SD. (**A**) A significant increase from Sham group is denoted by * ($p<0.01$), a significant increase from I/R group is denoted by ** ($p<0.01$) and a significant increase from BMP-2 group is denoted by *** ($p<0.01$). (**B**) A significant increase from Sham group is denoted by * ($p<0.01$), a significant increase from I/R group is denoted by ** ($p<0.01$), and a significant increase from I/R group is denoted by *** ($p<0.01$). (**C**) A significant increase from Sham group is denoted by * ($p<0.01$), a significant increase from I/R group is denoted by ** ($p<0.01$) and a significant increase from I/R group is denoted by *** ($p<0.01$).
Abbreviations: BMP-2, bone morphogenetic protein-2; Gli-1, glioma-associated oncogene-1; GA, glycyrrhetinic acid; HI/RI, hepatic ischemia/reperfusion injury; Ihh, Indian hedgehog; I/R, ischemia/reperfusion; PEG, poly(ethylene glycol); PLL, poly(L-lysine); Shh, sonic hedgehog; SD, standard deviation.

short half-life limit its applications.[17] Therefore, to design a delivery system for BMP-2 for HI/RI treatment is of great interest. In the present study, BMP-2 was loaded in PEG-b-PLL and GA-PEG-b-PLL via electrostatic interactions, and a spherical structure was formed (Figure 4A). The size of the BMP-2/PEG-b-PLL PIC micelle was approximately 62 nm, and the encapsulating capacity was 5.78% (Table 1).

In rats, a number of anti-HI/RI drugs could not achieve ideal therapeutic result due to fast clearance, poor permeability and short half-life, resulting in drug degradation and poor therapeutic activity.[17,51] Thus, in order to improve the biological activity and utilization rate of drugs, in this study, GA was attached on the surface of PEG-b-PLL PIC micelle as the liver-targeting ligand to accumulate drug in hepatocytes. Previous researches have shown that GA could be identified via GA receptor on hepatocyte membranes to impel drug uptake and higher accumulation in hepatic cells.[51,52] According to the in vitro transfection results in hepatic cells (Figure 4C), more fluorescence was exhibited by L-02 cells after incubation with GA-PEG-b-PLL PIC micelles. It was identified that the GA-PEG-b-PLL PIC micelle had a high affinity to L-02 cells than PEG-b-PLL PIC micelle did. High fluorescence of GA-PEG-b-PLL PIC micelle in L-02 cells also showed that GA would benefit the hepatic cells delivery, leading to encapsulation of higher concentration of drug in GA-PEG-b-PLL PIC micelle.

To improve and maintain anti-HI/RI actions after loading has been the prerequisite for developing drug delivery systems. Both the increase in liver cell uptake and sustained drug release offer a synergistic effect on anti-HI/RI.

The cytotoxicity assessment (Figure 4B) of PEG-b-PLL and GA-PEG-b-PLL against L-02 cells showed that the micelles exerted low cell toxicity.

HI/RI is a very complex process involving the production of oxygen free radicals, calcium overload, neutrophil infiltration, apoptosis, vascular endothelial damage and other pathophysiological processes, including many inflammatory mediators and immune factors. Previous studies have shown that TNF-α, IL-6 and MIP-2 inflammatory cytokines and oxidative stress injury significantly increased HI/RI.[46,53] Some studies have affirmed that BMP-2 reduced TNF-α, IL-6 and oxidative stress injury in I/R injury.[15,16] In this study, BMP-2, BMP-2/PEG-b-PLL and BMP-2/GA-PEG-b-PLL decreased TNF-α, IL-6 and MIP-2 inflammatory cytokines and oxidative stress injury in HI/RI (Figure 6B–D). Hedgehog (Hh) signaling pathway is a cellular communication playing an important role in animal development and regulates the renewal and proliferation of many adult tissues, organs and stem cells, and maintains morphology and function of normal tissues and organs.[54] During tissue and organ damage, Hh signaling pathway is activated to promote differentiation and proliferation of tissues and stem cells to repair injury.[55] Many documents have testified that expressions of Ki-67, Ihh, Shh and Gli-1 from Hh signaling pathway increase to promote liver regeneration in HI/RI and liver injury.[54,56] In this current study, BMP-2, BMP-2/PEG-b-PLL and BMP-2/GA-PEG-b-PLL further increased expressions of Ki-67, Ihh, Shh and Gli-1 to enhance liver regeneration in HI/RI (Figures 7 and 8). These results showed that GA-PEG-b-PLL as a BMP-2 delivery system could exhibit stable drug release and significant anti-HI/RI effects via liver targeting.

Conclusion

This was the first study to synthesize GA-PEG-b-PLL which can significantly improve the bioactivity and short half-life of BMP-2, and increase liver targeting. In addition, it demonstrated that BMP-2, BMP-2/PEG-b-PLL and BMP-2/GA-PEG-b-PLL preconditioning was capable of attenuating HI/RI, and BMP-2/GA-PEG-b-PLL preconditioning significantly reduced HI/RI through downregulating inflammatory factors, decreasing oxidative stress injury and modulating Hh signaling.

Acknowledgment

This work was financially supported by the Science and Technology Planning Project of Jiaxing, Zhejiang Province (2017AY33076).

Author contributions

All authors contributed toward data analysis, drafting and critically revising the paper and agree to be accountable for all aspects of the work.

Disclosure

The authors report no conflicts of interest in this work.

References

1. Tsung A, Hoffman RA, Izuishi K, et al. Hepatic ischemia/reperfusion injury involves functional TLR4 signaling in nonparenchymal cells. *J Immunol*. 2005;175(11):7661–7668.
2. Lemasters JJ, Thurman RG. Reperfusion injury after liver preservation for transplantation. *Annu Rev Pharmacol Toxicol*. 1997;37:327–338.
3. Sugawara Y, Kubota K, Ogura T, et al. Increased nitric oxide production in the liver in the perioperative period of partial hepatectomy with Pringle's maneuver. *J Hepatol*. 1998;28(2):212–220.
4. Trocha M, Merwid-Lad A, Chlebda E, et al. Influence of ezetimibe on selected parameters of oxidative stress in rat liver subjected to ischemia/reperfusion. *Acta Med*. 2014;10(4):817–824.
5. Gendy AM, Abdallah DM, El-Abhar HS. The potential curative effect of rebamipide against hepatic ischemia/reperfusion injury. *Naunyn Schmiedebergs Arch Pharmacol*. 2017;390(7):691–700.
6. Fondevila C, Busuttil RW, Kupiec-Weglinski JW. Hepatic ischemia/reperfusion injury – a fresh look. *Exp Mol Pathol*. 2003;74(2):86–93.
7. Wanner GA, Ertel W, Müller P, et al. Liver ischemia and reperfusion induces a systemic inflammatory response through Kupffer cell activation. *Shock*. 1996;5(1):34–40.
8. Malhi H, Gores GJ, Lemasters JJ. Apoptosis and necrosis in the liver: a tale of two deaths? *Hepatology*. 2006;43(2 Suppl 1):S31–S44.
9. Montalvo-Jave EE, Escalante-Tattersfield T, Ortega-Salgado JA, Piña E, Geller DA. Factors in the pathophysiology of the liver ischemia-reperfusion injury. *J Surg Res*. 2008;147(1):153–159.
10. Yang J, Shi P, Tu M, et al. Bone morphogenetic proteins: relationship between molecular structure and their osteogenic activity. *Food Sci Hum Wellness*. 2014;3(3–4):127–135.
11. Ma L, Lu MF, Schwartz RJ, Martin JF. Bmp2 is essential for cardiac cushion epithelial–mesenchymal transition and myocardial patterning. *Development*. 2005;132(24):5601–5611.
12. Hogan BL. Bone morphogenetic proteins: multifunctional regulators of vertebrate development. *Genes Dev*. 1996;10(13):1580–1594.
13. Padgett RW, Patterson GI. New developments for TGFbeta. *Dev Cell*. 2001;1(3):343–349.
14. Wang YX, Qian LX, Liu D, et al. Bone morphogenetic protein-2 acts upstream of myocyte-specific enhancer factor 2a to control embryonic cardiac contractility. *Cardiovasc Res*. 2007;74(2):290–303.
15. Ebelt H, Hillebrand I, Arlt S, et al. Treatment with bone morphogenetic protein 2 limits infarct size after myocardial infarction in mice. *Shock*. 2013;39(4):353–360.
16. Yang S, Pei L. [Influence of rhBMP-2 on the renal tissue of rat with renal ischemia reperfusion injury and its molecular mechanism]. *Yao Xue Xue Bao*. 2009;44(10):1089–1094. Chinese [with English abstract].
17. Jung T, Lee JH, Park S, et al. Effect of BMP-2 delivery mode on osteogenic differentiation of stem cells. *Stem Cells Int*. 2017;2017:7859184.
18. Chaturvedi K, Ganguly K, Nadagouda MN, Aminabhavi TM. Polymeric hydrogels for oral insulin delivery. *J Control Release*. 2013;165(2):129–138.
19. Wang J, Xu M, Cheng X, et al. Positive/negative surface charge of chitosan based nanogels and its potential influence on oral insulin delivery. *Carbohydr Polym*. 2016;136:867–874.
20. Lee DY, Choe K, Jeong YJ, et al. Establishment of a controlled insulin delivery system using a glucose-responsive double-layered nanogel. *RSC Adv*. 2015;5(19):14482–14491.

21. Mukhopadhyay P, Sarkar K, Bhattacharya S, Bhattacharyya A, Mishra R, Kundu PP. pH-Sensitive N-succinyl chitosan grafted polyacrylamide hydrogel for oral insulin delivery. *Carbohydr Polym*. 2014;112:627–637.
22. Gao X, Cao Y, Song X, et al. Biodegradable, pH-responsive carboxymethyl cellulose/poly(acrylic acid) hydrogels for oral insulin delivery. *Macromol Biosci*. 2014;14(4):565–575.
23. Gu Z, Dang TT, Ma M, et al. Glucose-responsive microgels integrated with enzyme nanocapsules for closed-loop insulin delivery. *ACS Nano*. 2013;7(8):6758–6766.
24. Mukhopadhyay P, Mishra R, Rana D, Kundu PP. Strategies for effective oral insulin delivery with modified chitosan nanoparticles: a review. *Prog Polym Sci*. 2012;37:1457–1475.
25. Lim HP, Tey BT, Chan ES. Particle designs for the stabilization and controlled-delivery of protein drugs by biopolymers: a case study on insulin. *J Control Release*. 2014;186:11–21.
26. Liu L, Zhou C, Xia X, Liu Y. Self-assembled lecithin/chitosan nanoparticles for oral insulin delivery: preparation and functional evaluation. *Int J Nanomedicine*. 2016;11:761–769.
27. Fonte P, Araújo F, Silva C, et al. Polymer-based nanoparticles for oral insulin delivery: revisited approaches. *Biotechnol Adv*. 2015;33(6 Pt 3):1342–1354.
28. Shan W, Zhu X, Liu M, et al. Overcoming the diffusion barrier of mucus and absorption barrier of epithelium by self-assembled nanoparticles for oral delivery of insulin. *ACS Nano*. 2015;9(3):2345–2356.
29. Zhang Y, Du X, Zhang Y, et al. Thiolated eudragit-based nanoparticles for oral insulin delivery: preparation, characterization, and evaluation using intestinal epithelial cells in vitro. *Macromol Biosci*. 2014;14(6):842–852.
30. Li X, Guo S, Zhu C, et al. Intestinal mucosa permeability following oral insulin delivery using core shell corona nanolipoparticles. *Biomaterials*. 2013;34(37):9678–9687.
31. Niu M, Lu Y, Hovgaard L, et al. Hypoglycemic activity and oral bioavailability of insulin-loaded liposomes containing bile salts in rats: the effect of cholate type, particle size and administered dose. *Eur J Pharm Biopharm*. 2012;81(2):265–272.
32. Xiong XY, Li QH, Li YP, Guo L, Li ZL, Gong YC. Pluronic P85/poly(lactic acid) vesicles as novel carrier for oral insulin delivery. *Colloids Surf B Biointerfaces*. 2013;111:282–288.
33. Nguyen VT, De Pauw-Gillet MC, Sandre O, Lauthier M. Biocompatible polyion complex micelles synthesized from arborescent polymers. *Langmuir*. 2016;32(50):13482–13492.
34. Zheng C, Gao H, Yang DP, et al. PCL-based thermo-gelling polymers for in vivo delivery of chemotherapeutics to tumors. *Mater Sci Eng C Mater Biol Appl*. 2017;74:111–116.
35. Lee Y, Kataoka K. Biosignal-sensitive polyion complex micelles for the delivery of biopharmaceuticals. *Soft Matter*. 2009;5(20):3810–3817.
36. Li N, Li XR, Zhou YX, et al. The use of polyion complex micelles to enhance the oral delivery of salmon calcitonin and transport mechanism across the intestinal epithelial barrier. *Biomaterials*. 2012;33(34):8881–8892.
37. Ishii S, Kamiya J, Nagasaki Y. Development of a long-acting, protein-loaded, redox-responsive, injectable gel formed by a polyion complex for local protein therapeutics. *Biomaterials*. 2016;84:210–218.
38. Kawamura A, Kojima C, Iijima M, et al. Polyion complex micelles formed from glucose oxidase and comb-type polyelectrolyte with poly(ethylene glycol) grafts. *J Polym Sci A Polym Chem*. 2008;46(11):3842–3852.
39. Negishi M, Irie A, Nagata N, Ichikawa A. Specific binding of glycyrrhetinic acid to the rat liver membrane. *Biochim Biophys Acta*. 1991;1066(1):77–82.
40. Zhang J, Zhang M, Ji J, et al. Glycyrrhetinic acid-mediated polymeric drug delivery targeting the acidic microenvironment of hepatocellular carcinoma. *Pharm Res*. 2015;32(10):3376–3390.
41. Huang W, Wang W, Wang P, et al. Glycyrrhetinic acid-modified poly(ethylene glycol)-b-poly(gamma-benzyl l-glutamate) micelles for liver targeting therapy. *Acta Biomater*. 2010;6(10):3927–3935.
42. Tong F, Tang X, Li X, Xia W, Liu D. The effect of insulin-loaded linear poly(ethylene glycol)-brush-like poly(l-lysine) block copolymer on renal ischemia/reperfusion-induced lung injury through downregulating hypoxia-inducible factor. *Int J Nanomedicine*. 2016;11:1717–1730.
43. Yu Y, Li S, Wang Z, et al. Interferon regulatory factor-1 activates autophagy to aggravate hepatic ischemia-reperfusion injury via the P38/P62 pathway in mice. *Sci Rep*. 2017;7:43[illegible]4.
44. Tong F, Dong B, Chai R, et al. Simvastatin nanoparticles attenuated intestinal ischemia/reperfusion injury by downregulating PAP4/COX-2 pathway in rats. *Int J Nanomedicine*. 201[illegible]2:2477–248[illegible]
45. Wang L, Li N, Lin D, Zan[illegible]. Curcumin protects against hepatic ischemia/reperfusion induced injury through inhibiting TLR4/NF-κB pathway. *Oncotarget*. 20[illegible]8:654[illegible]65420.
46. Ocuin LM, Zeng S, [illegible]wnar [illegible]. Nilotinib protects the murine liver from ischemia/reperfusion injury. *J Hepatol*. 2012;57(4):766–773.
47. Rebolledo RA, [illegible]rp AC, Ottens [illegible]ersema-Buist J, Leuvenink HG, Romanque [illegible]. Anti-apoptotic effects of 3,3′,5-triiodo-l-thyronine in the liver of brain-dead rats. *PloS One*. 2015;10(10):e0138749.
48. Ma[illegible] D, Infante P, Colicchia V, et al. PCAF ubiquitin ligase activity inhibits Hedgehog/Gli1 signaling in p53-dependent response to genotoxic stress. *Cell Death Differ*. 2013;20(12):1688–1697.
49. [illegible] Y, Huang Y, [illegible] J, Chen F, He Y, Zhang W. Role of Hedgehog-Gli1 signaling in the enhanced proliferation and differentiation of MG63 cells [illegible] by hierarchical micro-/nanotextured topography. *Int J Nanomedicine*. 2017;12:3267–3280.
50. [illegible] Li W, Li C, et al. Small hepatocyte-like progenitor cells may be a Hedgehog signaling pathway-controlled subgroup of liver stem cells. *Exp Ther Med*. 2016;12(4):2423–2430.
51. Smith JS, Xu Z, Byrnes AP. A quantitative assay for measuring clearance of adenovirus vectors by Kupffer cells. *J Virol Methods*. 2008;147(1):54–60.
52. Tian Q, Wang XH, Wang W, Zhang CN, Wang P, Yuan Z. Self-assembly and liver targeting of sulfated chitosan nanoparticles functionalized with glycyrrhetinic acid. *Nanomedicine*. 2012;8(6):870–879.
53. Tao YE, Wen Z, Song Y, Wang H. Paeoniflorin attenuates hepatic ischemia/reperfusion injury via anti-oxidative, anti-inflammatory and anti-apoptotic pathways. *Exp Ther Med*. 2016;11(1):263–268.
54. Yang JX, Jin H, Feng ZY, et al. [Effect of ischemia and reperfusion on expression of Hedgehog signaling in liver after rat partial hepatectomy]. *Chin J Exp Surg*. 2012;29:671–673. Chinese [with English abstract].
55. Omenetti A, Diehl AM. The adventures of sonic hedgehog in development and repair. II. Sonic hedgehog and liver development, inflammation, and cancer. *Am J Physiol Gastrointest Liver Physiol*. 2008;294(3):G595–G598.
56. Wang H, Zhang Y, Bai R, Wang M, Du S. Baicalin attenuates alcoholic liver injury through modulation of hepatic oxidative stress, inflammation and sonic hedgehog pathway in rats. *Cell Physiol Biochem*. 2016;39(3):1129–1140.

Supplementary material

Synthesis of GA-PEG-NH_2

Glycyrrhetinic acid (GA) was dissolved in dichloromethane, and then dicyclohexylcarbodiimide and N-hydroxysuccinimide (NHS) were added. The mixed solution was stirred for 8 h under N_2 protection, and N,N′-dicyclohexylurea was removed forming GA-NHS. The obtained GA-NHS and NH_2-poly(ethylene glycol) (PEG)-NH_2 were mixed in dichloromethane, and the mixture was stirred under N_2 protection for 24 h. The GA-PEG-NH_2 was finally obtained (Figure S1).

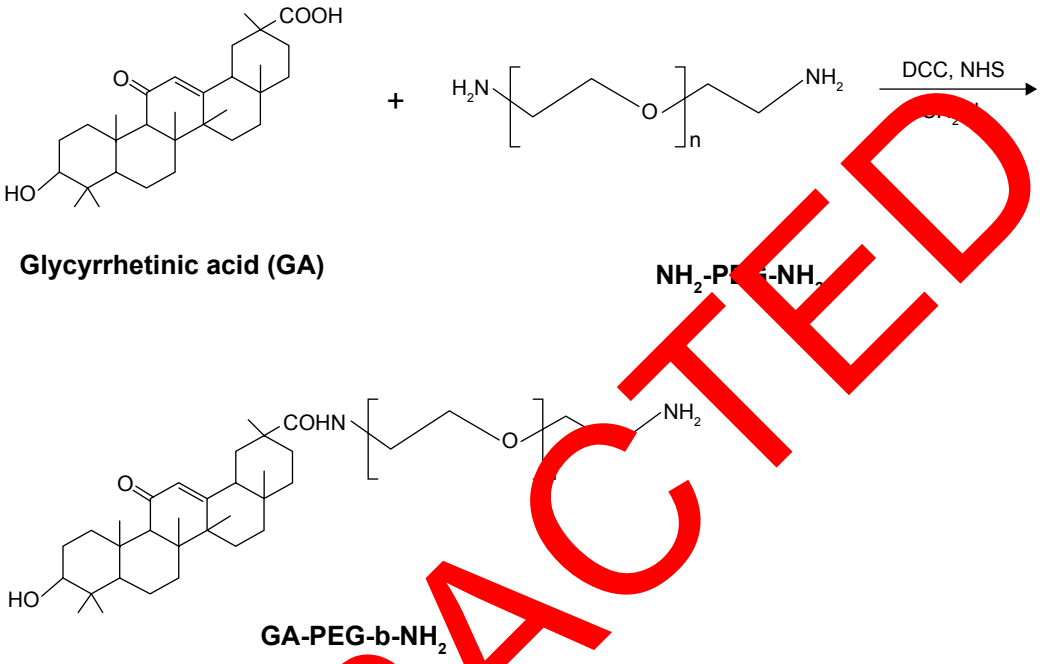

Figure S1 Synthesis of GA-PEG-NH_2.
Abbreviations: DCC, dicyclohexylcarbodiimide; GA, glycyrrhetinic acid; NHS, N-hydroxysuccinimide; PEG, poly(ethylene glycol).